Increasing the Hosting Capacity for Renewable Energy in Distribution Networks

Leonardo H. Macedo, John F. Franco, Rubén Romero
Department of Electrical Engineering
Sao Paulo State University
Ilha Solteira, Brazil
{leohfmp; jffranco}@gmail.com, ruben@dee.feis.unesp.br

Miguel A. Ortega-Vazquez
Department of Electrical Engineering
University of Washington
Seattle, United States
maov@uw.edu

Marcos J. Rider
Department of Systems and Energy
University of Campinas
Campinas, Brazil
mjrider@dsee.fee.unicamp.br

***Abstract*—Environmental concerns and the need to decarbonize the supply side of power systems are spurring the integration of renewable energy sources (RES). Consequently, an unprecedented increase of RES, particularly photovoltaic (PV) systems, has been observed in distribution grids. However, PV generation is weather-driven, and therefore its power production peak does not necessarily coincide with the peak demand. Therefore, large amounts of cheap renewable generation are usually spilled. This paper proposes a method for optimal allocation and sizing of energy storage systems (ESSs) to increase hosting capacity of PV generation in distribution networks. Moreover, network reinforcement and capacitor bank allocation are also considered. The problem is modeled using stochastic mixed-integer linear programming in which PV generation and demand are represented via scenarios. A 20-node test system is used to demonstrate the effectiveness of the proposed approach and to analyze the role of ESSs to improve the hosting capacity of RES.**

***Index Terms*—Distribution networks, energy storage, mixed-integer linear programming, photovoltaic generation, stochastic optimization.**

I. Introduction

The integration of renewable energy sources (RES), particularly photovoltaic (PV) generation, is rapidly increasing in modern distribution grids. The integration of cheap, renewable generation brings forth several advantages, including the environmental benefits, and technical advantages for distribution grids operation, among others. However, as any weather-driven source, PV generation is a function of solar irradiance, which does not coincide with heavy loading conditions in the grid, and thus the excess of generation is usually spilled. To maximize the utilization of renewable generation, the network must be upgraded using: i) conventional reinforcements, such as, replacement of conductors and by installing capacitor banks (CBs), and ii) emerging technologies, such as, by installing energy storage systems (ESSs). These investments would increase the hosting capacity of the system, i.e., the ability to integrate larger amounts of renewable generation to the system, while operating the grid within the technical limits. The investments in ESSs result in additional streams of benefits, including displacement of fossil-fueled generation, peak loading shaving, reduction of the operating cost of the system (charge with cheap electricity and discharge when electricity is expensive), and provision of ancillary services, among others.

Several works have proposed methods to allocate ESSs in distribution networks, to be able to integrate RES. Reference [1] is one of the first works to deal with this problem. The method presented is based on a heuristic, that uses an optimal power flow algorithm, which strives to optimize the location and size of ESSs to reduce the annual cost of energy purchased by the utility. In [2] a heuristic method, that uses the results of the discrete Fourier transform of the imbalance power, is used for sizing hybrid ESSs with different charging and discharging rates. A genetic algorithm is presented in [3] to integrate ESSs in Smart Grids. The proposed method considers allocation and sizing of ESSs and CBs, and replacing existing conductors to minimize losses and investments costs. Since both load and renewable generation are modelled as deterministic variables, the results are vulnerable to deviations from forecasted quantities, and thus the equipment selection is not only under- or over-sized, but potentially misplaced. A heuristic approach is presented in [4], with the objective of improving the hosting capacity in a subtransmission system by installing ESSs. A fuzzy particle swarm optimization algorithm is proposed in [5], where the objective is to reduce risks for the distribution system operator in a market framework, by sizing and siting ESSs. A mixed-integer second order cone programming model is presented in [6], and a genetic algorithm is presented in [7], for the allocation of ESSs in distribution networks for improved operation of the system. A hybrid tabu search/particle swarm algorithm is presented in [8] in order to determine the optimal storage planning in distribution networks with wind power generation. The tabu search is used to determine the optimal short-term operation planning of the distribution network, while the particle swarm algorithm determines the location and sizing of the ESSs. Reference [9] presents a mixed-integer nonlinear programming model for allocation of ESSs in distribution networks with high penetration of wind generation, and performs an analysis of the influence of the time-step discretization adopted. Reference [10] presents a method based in the fast Fourier transform to size an ESS composed by battery-supercapacitor to maintain the operation of isolated systems with high penetration of wind power.

To the best of the authors' knowledge, most of the papers propose heuristic and metaheuristic techniques to increase the hosting capacity of RES in distribution electrical power systems. Some common disadvantages of these approaches are

This work was supported by CNPQ, CAPES, and São Paulo Research Foundation (FAPESP), under grant 2016/10992-9.

978-1-5386-2890-4/17/$31.00 ©2017 IEEE

that they cannot guarantee optimality and that their parameters must be tuned to each problem. In addition, almost all works, are limited to determine investments decisions of ESSs. Since ESS is still an expensive technology [8], the benefits derived from their utilization should exceed their costs. Consequently, investments in conventional alternatives to reinforce the network should also be considered within the optimization problem, to attain minimum overall cost. This work proposes an approach to integrate large PV generation in distribution systems, by simultaneously considering conventional investments in reinforcements of the network as well as investing and allocating ESSs optimally. The uncertainties associated with the loads and PV generation are considered via stochastic programming. Furthermore, the nonlinearities associated with the representation of the operation of the system are linearized using conventional approaches. The resulting stochastic mixed-integer linear programming (MILP) model, that minimizes the investment and operating costs, is presented and discussed. Finally, the method is applied to solve a 20-node system, with various levels of PV generation penetrations.

II. Stochastic Model for the Problem

This section presents the proposed model for optimal network reinforcement and ESS investment. The optimization covers an operating period of $\overline{y}$ years (the set of years is $Y = \{1,2,\cdots,\overline{y}\}$) with a given load growth in each year. Since it is a mid-term planning problem, it is assumed that investment decisions are made at the outset of the simulation, and maintained over the whole optimization horizon. It should be noted, however, that the operation of the ESSs is optimized over the whole operating period.

A. Objective Function

The objective function (1) includes both the investment and operating costs. The investments in conductor replacement, CBs, and ESSs are the first-stage (here-and-now) decisions, while the operation of ESSs in the grid is a function of the scenario, therefore are second-stage decisions. For the operation, the present value of the annualized cost is considered.

$$\begin{aligned}\min \sum_{ij\in B}\sum_{a\in A} c^{br}_{\tau_{ij},a} l_{ij} w_{ij,a} + \sum_{i\in N}(c^{cb,fx} n^{cb}_i + c^{cb,i} q^{cb}_i) \\ + \sum_{i\in N}(c^{ess,P} P^{ess}_i + c^{ess,E} E^{ess}_i + c^{ess,i} h^{ess}_i) \\ + \sum_{i\in SE}\sum_{y\in Y}\sum_{s\in S}\sum_{t\in T}\left(\frac{1+\upsilon}{1+\alpha}\right)^{y-1} \psi \pi_s \delta_t (c^s_t P^{SE+}_{i,y,s,t} + c^b_t P^{SE-}_{i,y,s,t})\end{aligned} \quad (1)$$

The first term of (1) represents the investment costs of replacing conductors by others with greater capacity, in which B is the set of branches ij; A is the set of conductor types a; $c^{br}_{\tau_{ij},a}$ is the cost of replacing conductor of type τ_{ij} at branch ij by type a per unit of length; l_{ij} is the length of branch ij; and $w_{ij,a}$ is the binary variable that indicates the type of conductor a installed in branch ij. The second term represents the investment costs in CBs, where N is the set of nodes i; $c^{cb,fx}$ is the fixed cost of a CB module; $c^{cb,i}$ is the installation cost of a CB; n^{cb}_i is an integer variable that indicates the number of CB modules at node i; and q^{cb}_i is a binary variable that indicates the presence of a CB at node i.

The third term represents investments in ESSs, where the parameter $c^{ess,P}$ is the per unit cost of the power converter of an ESS; $c^{ess,E}$ is the per unit cost of the energy storage capacity for an ESS; $c^{ess,i}$ is the installation cost of an ESS; variable P^{ess}_i is the power rating of the ESS at node i; E^{ess}_i is the energy storage capacity of the ESS at node i; and h^{ess}_i is the binary variable that indicates the presence of an ESS at node i.

The last term of (1) represents the annualized operating cost, where SE is the set of substations; S is the set of operation scenarios s; T is the set of discretized times t of a day; the parameters α and υ are the annual interest an inflation rates, respectively; ψ is the number of days in a year; π_s the realization probability of scenario s; δ_t the duration of each time interval t; c^s_t and c^b_t are the selling and buying costs of energy at the substation at time t; and the nonnegative variables $P^{SE+}_{i,y,s,t}$ and $P^{SE-}_{i,y,s,t}$ are the active power generation and reverse power flow of a substation at node i, year y, scenario s, time t.

B. Constraints

The equations presented in this subsection for the operation of distribution networks are based on the branch flow model presented in [11]. The active and reactive power balance equations are shown in (2) and (3), $\forall i \in N, y \in Y, s \in S, t \in T$:

$$\begin{aligned}\sum_{ki\in B}\sum_{a\in A} P_{ki,a,y,s,t} \\ - \sum_{ij\in B}\sum_{a\in A}(P_{ij,a,y,s,t} + R_a l_{ij} I^{sq}_{ij,a,y,s,t}) + P^{SE+}_{i,y,s,t} \\ P^{SE-}_{i,y,s,t} + P^{rs}_{i,y,s,t} - P^{cut}_{i,y,s,t} + P^{ess+}_{i,y,s,t} - P^{ess-}_{i,y,s,t} = P^{D}_{i,y,s,t}\end{aligned} \quad (2)$$

$$\begin{aligned}\sum_{ki\in B}\sum_{a\in A} Q_{ki,a,y,s,t} \\ - \sum_{ij\in B}\sum_{a\in A}(Q_{ij,a,y,s,t} + X_a l_{ij} I^{sq}_{ij,a,y,s,t}) + Q^{SE}_{i,y,s,t} \\ + Q^{cb} n^{cb}_i = Q^{D}_{i,y,s,t}\end{aligned} \quad (3)$$

where the parameters $P^D_{i,y,s,t}$ and $Q^D_{i,y,s,t}$ are the active and reactive demands at node i, year y, scenario s, and time t; $P^{rs}_{i,y,s,t}$ is the active generation of the RES at node i, year y, scenario s, time t; Q^{cb} is the reactive power of a CB module; and R_a and X_a are the resistance and reactance of conductor of type a per unit of length. The variables $P_{ij,a,y,s,t}$, $Q_{ij,a,y,s,t}$, and $I^{sq}_{ij,a,y,s,t}$ are the active and reactive power flows and square of the current magnitude in branch ij, conductor a, year y, scenario s, time t, respectively. The variables $P^{cut}_{i,y,s,t}$ and $Q^{SE}_{i,y,s,t}$ are the active renewable generation curtailed and the reactive power generation of a substation at node i, year y, scenario s, time t; and $P^{ess+}_{i,y,s,t}$ and $P^{ess-}_{i,y,s,t}$ are the active power injection and extraction of the ESS at node i, year y, scenario s, time t.

Kirchhoff's voltage law is enforced in constraints (4) and (5), $\forall ij \in B, y \in Y, s \in S, t \in T$:

$$\begin{aligned}V^{sq}_{i,y,s,t} - V^{sq}_{j,y,s,t} \\ = \sum_{a\in A}[2(R_a P_{ij,a,y,s,t} + X_a Q_{ij,a,y,s,t}) l_{ij} + Z^2_a l^2_{ij} I^{sq}_{ij,a,y,s,t}]\end{aligned} \quad (4)$$

$$\hat{I}^{sq}_{ij,y,s,t} V^{sq}_{j,y,s,t} = \hat{P}^2_{ij,y,s,t} + \hat{Q}^2_{ij,y,s,t} \quad (5)$$

978-1-5386-2890-4/17/$31.00 ©2017 IEEE

where the parameter Z_a is the impedance of conductor of type a per unit of length; the variable $V^{sq}_{i,y,s,t}$ is the square of the voltage magnitude at node i, year y, scenario s, time t. The variables $\hat{P}_{ij,y,s,t}$, $\hat{Q}_{ij,y,s,t}$, and $\hat{I}^{sq}_{ij,y,s,t}$ are the total active and reactive power flows and the square of the total current through branch ij, year y, scenario s, time t, and are defined in (6)–(8), respectively, $\forall ij \in B, y \in Y, s \in S, t \in T$.

$$\hat{P}_{ij,y,s,t} = \sum_{a \in A} P_{ij,a,y,s,t} \tag{6}$$

$$\hat{Q}_{ij,y,s,t} = \sum_{a \in A} Q_{ij,a,y,s,t} \tag{7}$$

$$\hat{I}^{sq}_{ij,y,s,t} = \sum_{a \in A} I^{sq}_{ij,a,y,s,t} \tag{8}$$

The voltage limits for the system are enforced in (9):

$$\underline{V}^2 \leq V^{sq}_{i,y,s,t} \leq \overline{V}^2 \qquad \forall i \in N, y \in Y, s \in S, t \in T \tag{9}$$

where the parameters $\underline{V}$ and $\overline{V}$ are the minimum and maximum voltage magnitudes allowed in the system.

Constraint (10) represents the current limit of a branch in terms of the conductor selected, while (11) and (12) limit the active and reactive power flows on the conductor selected $\forall ij \in B, a \in A, y \in Y, s \in S, t \in T$:

$$0 \leq I^{sq}_{ij,a,y,s,t} \leq 3\overline{I}^2_a w_{ij,a} \tag{10}$$

$$|P_{ij,a,y,s,t}| \leq \sqrt{3V}\,\overline{I}_a w_{ij,a} \tag{11}$$

$$|Q_{ij,a,y,s,t}| \leq \sqrt{3V}\,\overline{I}_a w_{ij,a} \tag{12}$$

where the $\overline{I}_a$ is the current capacity of conductor of type a.

Constraint (13) imposes that only one option of conductor is selected for each branch of the system, $\forall ij \in B$.

$$\sum_{a \in A} w_{ij,a} = 1 \tag{13}$$

The capacity of the transformer of the distribution substation is represented by (14), $\forall i \in SE, y \in Y, s \in S, t \in T$:

$$(V^n)^2 \hat{I}^{sq}_{ij,y,s,t} \leq \left(\overline{S}^{SE}_i\right)^2 \tag{14}$$

where the parameter V^n is the nominal voltage of the system and $\overline{S}^{SE}_i$ is the apparent capacity of substation at node i. Equation (14) can be applied directly if the substation is connected to the system by only one branch. Otherwise, a fictitious node connected to the previous substation node, by a single fictitious branch, can be used to represent it.

The maximum number of CB modules is limited by (15), while (16) limits ne number of CBs in the system:

$$0 \leq n^{cb}_i \leq \overline{n}^{cb} q^{cb}_i \qquad \forall i \in N \tag{15}$$

$$\sum_{i \in N} n^{cb}_i \leq \overline{n}^{sys} \tag{16}$$

where the parameters $\overline{n}^{cb}$ and $\overline{n}^{sys}$ are the maximum number of CBs modules at a node and CBs in the system, respectively.

The renewable generation spillage is modeled in (17).

$$0 \leq P^{cut}_{i,y,s,t} \leq P^{rs}_{i,y,s,t} \qquad \forall i \in N, y \in Y, s \in S, t \in T \tag{17}$$

The constraints that define the ESSs capacities and power ratings are presented in (18) and (19), respectively:

$$0 \leq E^{ess}_i \leq h^{ess}_i \overline{E}^{ess} \qquad \forall i \in N \tag{18}$$

$$0 \leq P^{ess}_i \leq h^{ess}_i \overline{P}^{ess} \qquad \forall i \in N \tag{19}$$

where the parameters $\overline{E}^{ess}$ and $\overline{P}^{ess}$ are the maximum energy storage capacity and the power rating allowed for an ESS.

Constraints (20)–(23) define the operation of the ESSs, according to the limits in (18) and (19), $\forall i \in N, y \in Y, s \in S, t \in T$:

$$0 \leq P^{ess+}_{i,y,s,t} \leq P^{ess}_i \tag{20}$$

$$0 \leq P^{ess-}_{i,y,s,t} \leq P^{ess}_i \tag{21}$$

$$\epsilon_{i,y,s,t} = \epsilon_{i,y,s,t-1} + \gamma^-_y \eta^{ess-} \delta_t P^{ess-}_{i,y,s,t} - \delta_t P^{ess+}_{i,y,s,t}/(\gamma^+_y \eta^{ess+}) - \gamma^\beta_y \beta^{ess} \delta_t \epsilon_{i,y,s,t-1} \tag{22}$$

$$\xi E^{ess}_i \leq \epsilon_{i,y,s,t} \leq \gamma^E_y E^{ess}_i \tag{23}$$

where β^{ess} is the self-discharge rate of the ESS, η^{ess-} and η^{ess+} are, respectively, the charge and discharge efficiencies of an ESS, ξ is the minimum state of charge (SoC) of an ESS, and γ^-_y, γ^+_y, γ^β_y, and γ^E_y are aging factors of an ESS on year y. To consider these fixed aging factors, is assumed that the ESS will be correctly dimensioned, with a full charge/discharge cycle per day. Note that the proposed approach can accommodate other degradation characteristics such as those presented in [12]. The variable $\epsilon_{i,y,s,t}$ represents the SoC of the ESS at node i, year y, scenario s, time t.

Constraint (24) enforces a maximum limit for the spilled energy from RES, $y \in Y, s \in S$:

$$\sum_{i \in N} \sum_{t \in T} \delta_t P^{cut}_{i,y,s,t} \leq \varrho \sum_{i \in N} \sum_{t \in T} \delta_t P^{rs}_{i,y,s,t} \tag{24}$$

where the parameter ϱ represents the maximum percentage of energy spilled from RES.

C. Linear Equivalent of the Model

Since (5) is nonlinear and with the purpose of obtaining an MILP model, (25)–(31) are used to approximate it:

$$(V^n)^2 \hat{I}^{sq}_{ij,y,s,t} = \sum_{\lambda=1}^{\Lambda} m_{ij,\lambda} \left(\Delta^{\hat{P}}_{ij,\lambda,y,s,t} + \Delta^{\widehat{Q}}_{ij,\lambda,y,s,t}\right) \tag{25}$$

$$\hat{P}^+_{ij,y,s,t} - \hat{P}^-_{ij,y,s,t} = \hat{P}_{ij,y,s,t} \tag{26}$$

$$\hat{Q}^+_{ij,y,s,t} - \hat{Q}^-_{ij,y,s,t} = \hat{Q}_{ij,y,s,t} \tag{27}$$

$$\hat{P}^+_{ij,y,s,t} + \hat{P}^-_{ij,y,s,t} = \sum_{\lambda=1}^{\Lambda} \Delta^{\hat{P}}_{ij,\lambda,y,s,t} \tag{28}$$

$$\hat{Q}^+_{ij,y,s,t} + \hat{Q}^-_{ij,y,s,t} = \sum_{\lambda=1}^{\Lambda} \Delta^{\widehat{Q}}_{ij,\lambda,y,s,t} \tag{29}$$

$$\forall ij \in B, y \in Y, s \in S, t \in T$$

$$0 \leq \Delta^{\hat{P}}_{ij,\lambda,y,s,t} \leq \Delta^{\hat{S}}_{ij} \tag{30}$$

$$0 \leq \Delta^{\widehat{Q}}_{ij,\lambda,y,s,t} \leq \Delta^{\hat{S}}_{ij} \tag{31}$$

$$\forall ij \in B, \lambda \in \Lambda, y \in Y, s \in S, t \in T$$

where the length of each block of the power flow linearization is calculated using $\Delta^{\hat{S}}_{ij} = \overline{V} \max_{a \in A} \overline{I}_a / \Lambda$ (for a fictitious branch

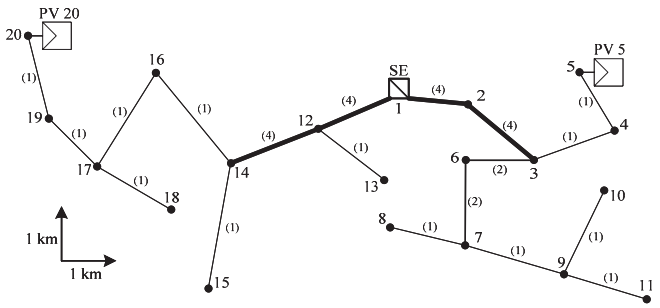

Figure 1. Modified 20-node distribution system.

used to represent an equivalent connection of a substation, $\Delta_{ij}^{\hat{S}} = \overline{S}_i^{SE}/\Lambda$), in which Λ is the number of blocks of the linearization, and the slope of each block is $m_{ij,1} = (5/6)\Delta_{ij}^{\hat{S}}$ and $m_{ij,\lambda} = (2\lambda - 1)\Delta_{ij}^{\hat{S}}$, for $\lambda > 1$.

The voltage magnitude (left-hand side of (5)) is replaced by the nominal voltage of the system, while its right-hand side is approximated by the piecewise linearization shown on the right-hand side of (25) and (26)–(31). Each total power flow variable $\hat{P}_{ij,y,s,t}$ and $\hat{Q}_{ij,y,s,t}$ is represented in (26) and (27) by two nonnegative variables $\hat{P}^{+}_{ij,y,s,t}$ and $\hat{P}^{-}_{ij,y,s,t}$, and $\hat{Q}^{+}_{ij,y,s,t}$ and $\hat{Q}^{-}_{ij,y,s,t}$, respectively. Equations (28) and (29) represent the absolute values of the power flow variables as a sum of the discretization variables $\Delta^{\hat{P}}_{ij,\lambda,y,s,t}$ and $\Delta^{\hat{Q}}_{ij,\lambda,y,s,t}$. Finally, the limits of each variable are defined in (30) and (31). It should be noted that greater values of Λ improve the accuracy of the linearization, but also increase the size and computational burden of the model. Thus, the MILP model defined by (1)–(4), (6)–(31) is a stochastic formulation for the allocation and sizing of ESSs and network reinforcement of distribution systems with high penetration of PV generation.

III. Tests and Results

The proposed stochastic MILP model is implemented in AMPL [13] and solved using CPLEX [14], on a computer with an Intel Core i7-4770 processor and 16 GB of RAM.

The 20-node distribution system, adapted from the 54-node distribution system [15], is used to test the proposed method. The topology of the modified 20-node distribution system is illustrated in Fig. 1. The values shown at each branch represent the initial conductor types τ_{ij}. The system has 19 load nodes, one substation and two PV generation units at nodes 5 and 20. The apparent capacity of the substation is $\overline{S}_i^{SE} = 20$ MVA and the nominal voltage is $V^n = 15$ kV. Complete data for the system is available in [16]. The general parameters for the simulations are: interest rate $\alpha = 10\%$, inflation rate $\upsilon = 7\%$ [8], duration of each time interval $\delta_t = 1$h, $\psi = 365$, number of blocks in the piecewise linearization $\Lambda = 10$, $\underline{V} = 0.95$ p.u., and $\overline{V} = 1.05$ p.u. A period of five years ($\overline{y} = 5$) with an annual load growth rate of 3% is assumed [8]. The technical specifications of the conductors considered are shown in Table I, while Table II shows the costs of replacing the conductors [15].

For the CBs, each module has reactive power capacity $Q^{cb} = 300$ kvar; a capital cost $c^{cb,fx} = 7500$ USD; and each node can accommodate a maximum of $\overline{n}^{cb} = 4$ CB modules. The installation cost of a CB is assumed to be $c^{cb,i} = 1600$ USD, and the maximum number of CBs in the system is $\overline{n}^{sys} = 5$ [17]. The parameters for the ESSs are: self-discharge ratio $\beta^{ess} = 0.002$/h, minimum SoC $\xi = 10\%$, $\eta^{ess+} = \eta^{ess-} = 93\%$, $c^{ess,E} = 225$ USD/kWh [8], unit cost of power rating for storage $c^{ess,P} = 175$ USD/kW [8], installation cost of an ESS $c^{ess,i} = 5000$ USD, $\overline{E}^{ess} = 8$ MWh, and $\overline{P}^{ess} = 2$ MW. The deterioration of the ESSs is assumed to be linear, and the aging factors are $\gamma_y^- = \gamma_y^+ = \gamma_y^E = 1 - 0.02y$ and $\gamma_y^\beta = 1 + 0.02y$ for year y [12].

TABLE I. Technical Specifications of the Conductors

Type a	R_a (Ω/km)	X_a (Ω/km)	$\overline{I}_a$ (A)
1	0.3655	0.2520	150
2	0.2921	0.2466	250
3	0.2359	0.2402	350
4	0.1932	0.2279	450

TABLE II. Costs $c^{br}_{\tau_{ij},a}$ of Replacing Conductor Type τ_{ij} by Conductor Type a (10^3 USD/km)

		To type a			
		1	2	3	4
From type τ_{ij}	1	0	34	41	44
	2	M	0	40	41
	3	M	M	0	40
	4	M	M	M	0

TABLE III. Solutions for Cases A1–A3

Case	A1: 100-45%	A2: 30%	A3: 20%
Conductor	3(16-17)	2(3-4), 2(4-5)	3(3-4), 4(4-5)
CB	3(7), 2(10), 1(16), 2(18)	1(7), 3(10), 3(17), 1(18)	3(10), 1(11), 1(17), 2(18), 1(19)
An. PV gen. (GWh)	24.03	27.92	31.90
Invest. (MUSD)	0.150	0.162	0.187
Oper. (MUSD)	25.643	25.786	25.961

Following, three cases that consider different alternatives to increase the RES hosting capacity of distribution systems are presented. The first one considers only conductor replacement and CB allocation, the second case considers only ESSs allocation and sizing, and the third case considers all these alternatives simultaneously.

A. Integrating PV Generation with Traditional Alternatives

Table III shows the results for three values of maximum percentage of energy spilled from RES, ϱ. For Case A1, no limit is considered (i.e., $\varrho = 1$), the maximum spilled energy is 45%. To achieve this, the conductor of branch 16-17, initially of type 1, is replaced by type 3. Also, three CB modules are installed at node 7, two at node 10, one at node 16, and two at node 18. The investment cost is 0.150 MUSD and the operation cost is 25.643 MUSD. Note that when higher levels of integration of PV energy are desired (Cases A2 and A3, with $\varrho = 0.3$ and $\varrho = 0.2$), more investment is made to ensure the feasible operation of the system. For each case, Table III also presents the average annual PV energy generation.

Although the investment costs for Cases A1–A3 are lower in comparison to Cases B and C (following sections), it must be noted that since energy cannot be stored to be consumed during the peak hours, the excess is sold through the substation with a lower price, resulting in higher operating costs.

978-1-5386-2890-4/17/$31.00 ©2017 IEEE

TABLE IV. SOLUTIONS FOR CASES B1–B3

Case	B1: 100-37%	B2: 30%	B3: 25%
ESS	3.08/0.67(10), 0.61/0.21(11), 5.67/0.95(20)	4.56/0.63(5), 2.73/0.60(10), 0.64/0.13(11), 6.63/0.96(20)	8.00/2.00(5), 2.57/0.44(10), 8.00/1.44(20)
An. PV gen. (GWh)	27.06	28.99	30.96
Invest. (MUSD)	2.447	3.706	4.872
Oper. (MUSD)	23.480	22.305	21.386

TABLE V. SOLUTIONS FOR CASES C1–C3

Case	C1: 100-42%	C2: 30%	C3: 20%
Conductor	–	4(17-19), 4(19-20)	3(3-4), 2(4-5), 4(6-7)
CB	2(10), 2(18)	2(18)	1(9), 1(18)
ESS	2.47/0.45(11), 2.29/0.38(20)	6.74/0.93(10), 2.02/0.30(18)	2.81/0.39(10), 6.81/0.98(20)
An. PV gen. (GWh)	25.09	28.71	31.95
Invest. (MUSD)	1.258	2.337	2.601
Oper. (MUSD)	24.529	23.609	23.525

B. Integrating PV Generation with ESS

In this case, only investment in ESS is considered. Three subcases are considered again (see Table IV), Case B1 with $\varrho = 1$, Case B2 with $\varrho = 0.3$, and Case B3 with $\varrho = 0.25$. For Case B1, a maximum of 37% of renewable energy is spilled (for all scenarios in all years). To achieve this, three ESSs are installed in the system, one at node 10, with storage capacity of 3.08 MWh and power rating of 0.67 MW, other at node 11 (0.61 MWh/0.21 MW), and the last one at node 20 (5.67 MWh/0.95 MW) The investment cost is 2.447 MUSD and the operation cost is 23.480 MUSD. Higher levels of PV energy integration require more investments (3.706 MUSD for $\varrho = 0.3$, 4.872 MUSD for $\varrho = 0.25$), leading to lower operating costs. In Cases B1–B3, the feasible operation of the system is guaranteed by the ESSs, which improve the voltage profile and reduce congestions in the system due the presence of PV generation, with high investment costs. However, ESS are not capable of allowing higher penetrations of PV energy, i.e., for $\varrho < 0.25$, the problem becomes infeasible. To allow higher participations of PV generation, the network must be reinforced together with ESS allocation, as following.

C. Integrating PV Generation Considering All Alternatives

The results when reinforcements in the network and ESS sizing and allocation are considered simultaneously are presented in Table V. For Case C1, a maximum of 42% of renewable energy is spilled with an investment of 1.258 MUSD. Maximum levels of energy spilled of 30% and 20% can be achieved with investments of 2.337 MUSD and 2.601 MUSD, respectively (Cases C2 and C3). The investment costs for Cases C1–C3 are lower than for Cases B1–B3. Additionally, higher penetration of PV generation can be achieved, demonstrating the importance of performing an integrated analysis to improve the hosting capacity of distribution systems.

IV. CONCLUSION

A method to increase the hosting capacity of renewable energy sources (RES) in distribution networks is presented. The proposed approach optimizes over reinforcements considering conventional alternatives (e.g. replacement of conductors and allocation of capacitor banks) and installing energy storage systems (ESSs). The method chooses strategic solutions that minimize the overall operating costs for the utility. Each of these decisions compares reinforcements and auxiliary equipment (e.g. capacitor banks) against installing and operating ESSs in a mid-term optimization framework. The method considers the uncertainty of RES and load by means of scenarios, which are solved by a stochastic mixed-integer linear programming model.

The results show the effectives of the proposed approach, and stress the importance of strategic investments in ESSs simultaneously with conventional reinforcements, to allow larger penetration of RES in the distribution system.

REFERENCES

[1] Y. M. Atwa and E. F. El-Saadany, "Optimal allocation of ESS in distribution systems with a high penetration of wind energy," *IEEE Trans. Power Syst.*, vol. 25, no. 4, pp. 1815–1822, Nov. 2010.

[2] Y. V. Makarov, P. Du, M. C. W. Kintner-Meyer, C. Jin, and H. F. Illian, "Sizing energy storage to accommodate high penetration of variable energy resources," *IEEE Trans. Sustain. Energy*, vol. 3, no. 1, pp. 34–40, Jan. 2012.

[3] G. Carpinelli, G. Celli, S. Mocci, F. Mottola, F. Pilo, and D. Proto, "Optimal integration of distributed energy storage devices in smart grids," *IEEE Trans. Smart Grid*, vol. 4, no. 2, pp. 985–995, Jun. 2013.

[4] N. Etherden and M. H. J. Bollen, "Dimensioning of energy storage for increased integration of wind power," *IEEE Trans. Sustain. Energy*, vol. 4, no. 3, pp. 546–553, Jul. 2013.

[5] Y. Zheng, Z. Y. Dong, F. J. Luo, K. Meng, J. Qiu, and K. P. Wong, "Optimal allocation of energy storage system for risk mitigation of DISCOs with high renewable penetrations," *IEEE Trans. Power Syst.*, vol. 29, no. 1, pp. 212–220, Jan. 2014.

[6] M. Nick, R. Cherkaoui, and M. Paolone, "Optimal allocation of dispersed energy storage systems in active distribution networks for energy balance and grid support," *IEEE Trans. Power Syst.*, vol. 29, no. 5, pp. 2300–2310, Sep. 2014.

[7] A. S. A. Awad, T. H. M. El-Fouly, and M. M. A. Salama, "Optimal ESS allocation for load management application," *IEEE Trans. Power Syst.*, vol. 30, no. 1, pp. 327–336, Jan. 2015.

[8] M. Sedghi, A. Ahmadian, and M. Aliakbar-Golkar, "Optimal storage planning in active distribution network considering uncertainty of wind power distributed generation," *IEEE Trans. Power Syst.*, vol. 31, no. 1, pp. 304–316, Jan. 2016.

[9] S. W. Alnaser and L. F. Ochoa, "Optimal sizing and control of energy storage in wind power-rich distribution networks," *IEEE Trans. Power Syst.*, vol. 31, no. 3, pp. 2004–2013, May 2016.

[10] Y. Liu, W. Du, L. Xiao, H. Wang, S. Bu, and J. Cao, "Sizing a hybrid energy storage system for maintaining power balance of an isolated system with high penetration of wind generation," *IEEE Trans. Power Syst.*, vol. 31, no. 4, pp. 3267–3275, Jul. 2016.

[11] M. Farivar and S. H. Low, "Branch flow model: Relaxations and convexification-Part I," *IEEE Trans. Power Syst.*, vol. 28, no. 3, pp. 2554–2564, Aug. 2013.

[12] M. A. Ortega-Vazquez, "Optimal scheduling of electric vehicle charging and vehicle-to-grid services at household level including battery degradation and price uncertainty," *IET Gener. Transm. Distrib.*, vol. 8, no. 6, pp. 1007–1016, Jun. 2014.

[13] R. Fourer, D. M. Gay, and B. W. Kernighan, *AMPL: A Modeling Language for Mathematical Programming*, 2nd ed. Duxbury, MA, USA: Cengage Learning, 2002.

[14] ILOG, *CPLEX Optimization subroutine library guide and reference, version 11.0*. Incline Village, NV, USA, 2008.

[15] J. F. Franco, M. J. Rider, M. Lavorato, and R. Romero, "Optimal conductor size selection and reconductoring in radial distribution systems using a mixed-integer LP approach," *IEEE Trans. Power Syst.*, vol. 28, no. 1, pp. 10–20, Feb. 2013.

[16] "LaPSEE Power System Test Cases Repository," 2016. [Online]. Available: http://www.feis.unesp.br/#!/lapsee. [Accessed: 01-Dec-2016].

[17] A. Y. Abdelaziz and A. A. El-Fergany, "Efficient heuristic-based approach for multi-objective capacitor allocation in radial distribution networks," *IET Gener. Transm. Distrib.*, vol. 8, no. 1, pp. 70–80, Jan. 2014.

978-1-5386-2890-4/17/$31.00 ©2017 IEEE